This article is published online with Open Access by IOS Press and distributed under the terms of the Creative Commons Attribution Non-Commercial License 4.0 (CC BY-NC 4.0).

doi:10.3233/PMST250008

A CFD Based Method to Assess Underwater Venting of Methanol and Nitrogen for Yachts

First authors: Sara Rasori^{a,1}, Marco Falossi^a Co-authors: Filippo Bollentini^a, Federico Tocchi^a, Edward Canepa^b, Aris Twerda^c

^a Sanlorenzo spa

^b University of Genoa

^c TNO

Abstract. Methanol is a promising alternative fuel for maritime decarbonization, but current safety regulations are designed for large ships and pose challenges for yacht integration. A key issue is the venting of methanol vapours, which creates hazardous deck areas incompatible with yacht design. This study proposes an innovative solution: underwater venting during bunkering. Using CFD simulations in Star-CCM+ with Eulerian Multiphase modelling, we analyze vapor dispersion, dissolution (based on Henry's law), and safety implications. Results show that underwater venting effectively mitigates risks, ensuring regulatory compliance while enabling safer yacht designs.

Keywords. Methanol fuel, Yacht safety, Underwater venting, CFD simulation, Hazardous area

1. Introduction

Due to climate concerns, the maritime industry faces pressure to reduce its carbon footprint. For this reason, the International Maritime Organization (IMO) set an initial target of reducing total annual GHG emissions by at least 50% by 2050 compared to 2008 levels [1]. This was strengthened in July 2023 when the MEPC 80 meeting established a goal to reach net-zero GHG emissions by approximately 2050, with a 40% reduction by 2030 [2]. Although not covered by IMO regulation on GHG reduction, in this context, the luxury yacht industry faces the complex challenge of pursuing a trade-off between premium features and voluntary reduction of environmental impact.

An interesting step forward in this direction could be the adoption of renewable fuels [3] [4], among which methanol is emerging in a promising way in the maritime sector, leading to a 99% reduction in SO_x, a 60% reduction in NO_x, and up to 95% reduction in particulate matter compared to conventional marine fuels [5]. It necessitates specific safety measures [6]: It is toxic when ingested [7] or inhaled, the OSHA PEL is 200 ppm for an 8-hour workday and a 40-hour workweek, while the STEL is 250 ppm, relative to a 15-minute period [8]. The IDLH concentration for methanol, as defined by the NIOSH, is 6,000 ppm [8]. Moreover, thanks to its liquid state at ambient temperature, methanol is more straightforward to use; bi-fuel systems powered by diesel and renewable methanol offer a good trade-off between carbon emissions reductions and volume

_

¹ Corresponding Author: Sara Rasori, s.rasori@sanlorenzoyacht.com

required by machinery and fuel [9]. This article proposes a CFD - based method for risk assessment of hazardous areas during underwater venting in methanol refuelling.

2. Case study

This study examines a 500 GT 50 m Sanlorenzo luxury yacht under construction, powered by two bi-fuel engines with two bi-fuel gensets for onboard electricity production, enabling the use of a mixture of conventional diesel fuel and green methanol. As part of the LIFE MYSTIC EU co-funded project (Project ID: 101148420 Acronym: LIFE23-ENV-IT-LIFE MYSTIC), this vessel represents an application of alternative fuels in the maritime sector, leading to an important reduction of GHG emissions compared to conventional diesel-only systems [10].

Venting during refuelling phase of the methanol tank, inerted with nitrogen directly produced on board, is analysed in this study. Inside the tank above the liquid surface, a mixture of nitrogen and methanol vapour is present. In order to evaluate the composition of the gas phase, methanol's vapor saturation pressure is considered [11]. For the sake of any safety concern, the analysis is performed considering a conservative condition where the mixture is always saturated by methanol vapour, not accounting for any eventual stratification or time evolution of diffusion effects inside the tank.

The venting system includes a spring-loaded valve that opens at a reference internal pressure, connected to a pipe that extends underwater. A temperature of 20 °C is considered, in these conditions a relief of a 11%vol methanol vapor and 89%vol nitrogen mixture is expected. During refuelling, as liquid methanol enters the tank, the gas phase is compressed until the valve opens, releasing the mixture underwater before closing as pressure decreases, creating a cyclic process.

A cyclic underwater relief of a mixture containing methanol vapor from the boat suggests the need for an investigation regarding safety conditions. Although a very strong dissolution is expected [12], which should lead to negligible concentrations in the air above the water surface, the release conditions might affect the ongoing phenomena.

3. Numerical modelling

The chosen numerical model to perform the risk assessment of underwater venting is the Eulerian Multiphase (EMP) in Star CCM+ based on a Eulerian – Eulerian formulation where each distinct phase has its own set of conservation equations [13].

In the flow where the particles in the dispersed phase are bubbles, the size of the bubbles can change continuously due to breakup and coalescence phenomena. At the base of the method there's the Population Balance Equation (PBE) [14]:

$$\frac{\partial n(d_p)}{\partial t} + \nabla \cdot \left(vn(d_p) \right) = B - D$$

Where:

- $n(d_p)$ is the particle number density which gives the number of particles with diameters from d_p to $d_p + d(d_p)$
- B, D are the birth and death terms due to breakup, coalescence, nucleation, dissolution.

The population balance model chosen for this case is the S-Gamma model defined also as the method of moments.

For breakup, the model considers the balance between disruptive forces due to shear and turbulence and restoring forces due to surface tension on the particle.

The breakup rate is defined as [15]:

Breakup rate =
$$C_g \frac{\left(\epsilon_f d_p\right)^{\frac{1}{3}}}{d_n} f\left(\frac{We_{cr}}{We}\right)$$

Where:

- C_g is the constant calibration
- We is the Weber number and We_{cr} is the critical Weber number
- d_p is the droplet diameter
- ε_f is the turbulence dissipation rate of the continuous phase

For the coalescence, the model considers the probability of collisions of the particles, the contact time of two colliding particles and the drainage time of fluid film between the particles.

The coalescence rate is defined as:

Coalescence rate =
$$h \cdot \lambda$$

Where:

- h is the collision rate between two droplets
- λ is the coalescence efficiency

$$\lambda = \exp\left(-C\frac{t_{rupture}}{t_{contact}}\right)$$

where:

- C is the calibration constant (higher values of C reduce the probability of coalescence)
- $t_{contact}$ is the contact time
- $t_{rupture}$ is the time needed for breakup

The assumption at the base of the S-Gamma model conforms to a pre-defined shape function (**log normal**).

$$P(d_P) = \frac{1}{d_n \sigma \sqrt{2\pi}} \exp\left(-\frac{\ln(d_p) - \mu)^2}{2\sigma^2}\right)$$

Where:

- d_p is the particle diameter
- P(d_p) is the probability density function of particle diameter
- μ is the mean logarithm of particle diameter
- σ is the standard deviation of particle diameter

4. Setup of the simulation

The simulation domain (Figure 1) has been created basing on a portion of the yacht hull located close to the stern, where the venting phenomenon is taking place. Such a yacht portion extends longitudinally for 10 m from the stern, while the numerical domain starts 3 m astern. The domain has been divided in two regions: water (in blue in Figure 2) and air (in green in Figure 2). In both the regions, all the boundaries, except from the venting

inlet and the hull surface, are defined as hydrostatic pressure outlet. The venting inlet (circled in the Figure 2) is defined as a velocity inlet.



Figure 1. 3D model created in Rhinoceros (yacht hull in grey and the considered numerical domain in blue).

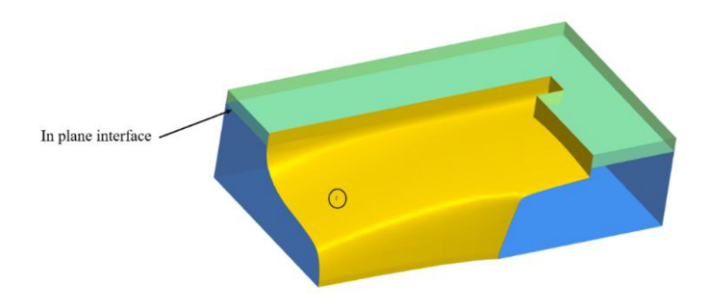


Figure 2. Domain composed by water and air regions

The two regions are connected through an interface, indicated with an arrow in Figure 2, with imprinted connectivity. The grid is composed by trimmed cells with a 0.01 m base size. On the hull surface a prism layer mesh has been adopted (10 layers with a minimum wall distance equal to 0.005 m). A local refinement has been introduced to better resolve the complex flow in the gas mixture injection area. The grid is composed by 2.3 M cells ad it is shown in Figure 3.

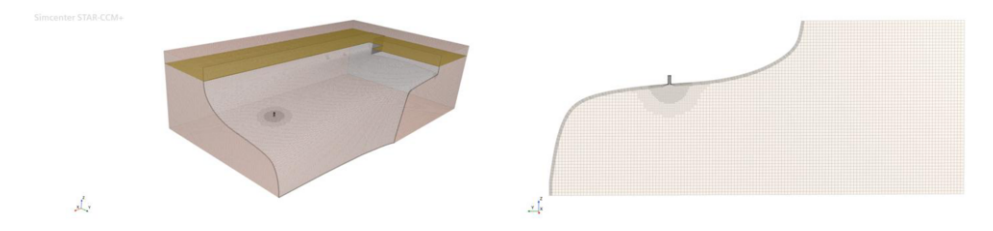


Figure 3.Mesh of the domain

On inlet boundary, representing the outlet section of the venting pipeline, the wall normal flow velocity has been imposed as well as the gas composition. The inlet gas mixture is composed of nitrogen and methanol vapour with mole fractions equal to 0.893 and 0.107 respectively. The inlet flow Sauter mean diameter has been defined equal to 5 mm. Three values of the inlet flow velocity have been investigated, specifically 2 m/s, 10 m/s and 70 m/s. Such values have been defined as representative of three different venting procedures. In the present study only the 70 m/s case results will be discussed. Nevertheless, such a condition turns out to be the most precautionary taking into

consideration the objective of the study, namely, to propose a methodology for risk assessment in the case of underwater venting.

5. Settings

Implicit URANS second order numerical scheme have been used with k- ϵ turbulence model and wall functions for effective boundary layer resolution.

The liquid phase is a Multi-Component Liquid composed of methanol, water and nitrogen and the gas phase it is a multi-component gas composed by water and methanol. The continuous phase is the liquid phase while the dispersed phase is the gas one.

To characterize the initial particle size distribution in the dispersed phase a Sauter Mean Diameter (SMD) [16] of 5 mm is chosen as first attempt value.

The parameters required by the model for the correct simulation of dissolution are Henry's constant and Sherwood number (Sh).

For the continuous phase, the Sherwood number is locally calculated with the use of Ranz-Marshall correlation [17].

$$Sh_{continous\ phase} = 2 + 0.6Re^{1/2}Sc^{1/3}$$

Where:

- Re is the Reynolds Number
- Sc is the Schmidt number

For the dispersed phase, the Sherwood number has been valuated instead utilizing the following formula [12]:

$$Sh = 1 + (1 + Pe)^{0.33} \left(1 + \frac{0.096Re^{0.33}}{1 + 7Re^{-2}} \right)$$

Where:

- Pe is the Peclet Number
- Re is the Reynolds Number

In Table 1 are reported the main settings utilized to set up the simulation.

Initial Sauter mean Diameter [mm] 5

Continuous Phase Sherwood Number Ranz-Marshall Law
Dispersed Phase Sherwood Number 18

Henry's Law Coefficient for Methanol [bar] 0.14187

Henry's Law Coefficient for Nitrogen [bar] 59500

Time-step [s] 0.005

Table 1. Main simulation's settings

6. Post-processing

The plume that protrudes in the water due to a venting phenomenon at 70m/s is shown in pink in Figure 4; since the bottom surface it is not so inclined with respect to the horizontal plane, there's a short time in which there is an equilibrium between the capacity of the plume to aggregate all the particles due to its density and the effect of the buoyancy.

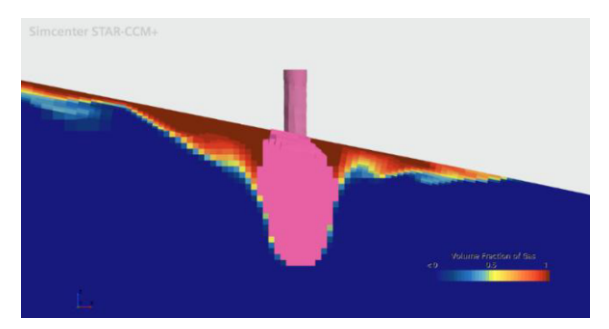


Figure 4. Protrusion of 30 cm at venting outlet, velocity: 70 m/s

In order to characterize the behaviour of the gas mixture along the path before reaching the surface, the underwater domain has been clustered applying a two steps approach. Initially a threshold on the volume fraction of gas (0.01) has been applied in the way to account for the gas presence. Secondarily, such a sub-dataset has been clustered basing on the distance from the inlet boundary. In this way the submerged cells having volume fraction of gas greater than 0.01 are sorted in circular strips as represented in Figure 5. The mean mass fraction of methanol vapour and its standard deviation have been evaluated for each dataset. This results in the distribution of the mean methanol vapour mass fraction as a function of the distance from the inlet which is reported in Figure 6. The mass fraction standard deviation curve, as well the maximum value one, have been added to the plot.



Figure 5. Underwater domain data clustering. (first data cluster based on the volume fraction of gas in pink, the circular strips in grey)

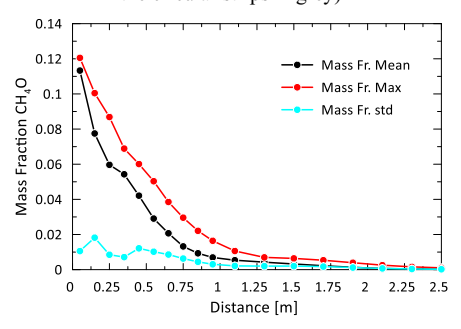


Figure 6. Distribution of the methanol vapour mass fraction.

The mean mass fraction curve indicates that, as the gas flow moves away from the inlet, the methanol vapour percentage is progressively reduced. In fact, considering that the inlet gas mixture is characterized by a methanol mass fraction equal to 0.121, after a

0.35 m path such a value reduces to 0.055. At a distance of 1 m the mean methanol mass fraction is around 0.007. Such a behaviour is confirmed by the curve related to the mass fraction maxima. The distribution of the standard deviation of the methanol mass fraction for each circular-strip-like dataset indicates a progressive reduction in the data spreading. The reduction in the methanol mass fraction may be ascribed to the vapour dissolution in water which appears to be extremely effective. Moreover, the standard deviation trend suggests that this mechanism is strongly deterministic. Similar results may be obtained performing a weighted averaging process based on the Sauter mean diameter or on the cell gas phase volume.

In order to highlight the dissolution mechanism qualitatively, the instantaneous data has been used to compute the methanol vapour mass flow rate crossing the free surface. Such a quantity is equal to 6.13×10^{-6} kg/s which may be compared to the inlet mass flow rate (0.03 kg/s).

Since the risk tables regarding the hazard levels of methanol are expressed in ppm, some probes have been placed at different positions within the domain (Table 2).

In the Figure 7 all the probes are plotted.

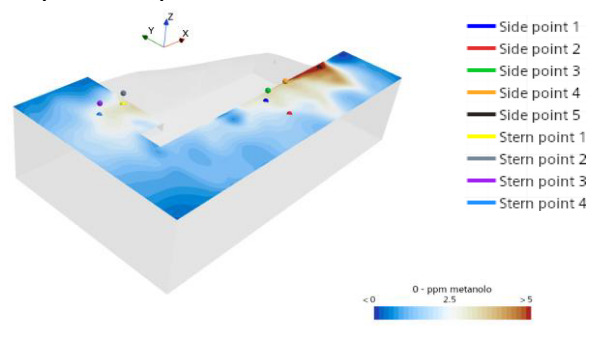


Figure 7. Display of the probes

All the PPM values are reported in Table 2:

Table 2. Vertical position of probes in the domain and corresponding PPM detected @ 70m/s of venting phenomena

Position	Stern				Side				
N° point	1	2	3	4	1	2	3	4	5
Z [m]	0.02	0.45	0.45	0.02	0.02	0.02	0.45	0.45	0.02
PPM	2.95	0.001	0.11	2.52	2.81	1.86	0.0007	0.074	5.60

7. Conclusions

The present work shows that methanol exhibits a high solubility in water, based on physical parameters and models available in referred literature. At the free surface, the concentration levels detected (ppm) are well below the lower threshold limits identified for long term exposure related to human health [8] [7]. The results ensure that there is no risk of exposure to harmful concentrations of methanol in the surrounding environment if this is confirmed by experimental validation.

Comparing these results with the ones obtained for other velocities, the main difference lies in the spatial distribution of the dissolution process. Specifically, higher velocities result in a greater dissolution length, meaning that methanol dissolves over a larger distance before reaching complete dispersion.

8. References

- [1] IMO, "Marine Environment Protection Committee (MEPC), 74th session, 13-17 May 2019," [Online].
- [2] IMO, "ANNEX 15, RESOLUTION MEPC.377(80), 2023 IMO STRATEGY ON REDUCTION OF GHG EMISSIONS FROM SHIPS," [Online].
- [3] DNV, "Assessment of selected alternative fuels and technologies in shipping," [Online].
- [4] IEA, "Transport biofuels," [Online].
- [5] Methanex, "Methanol as a marine fuel," [Online].
- [6] Carl Roth, "Methanol safety datasheet," [Online].
- [7] Methanol Institute, "Methanol Safe Handling Manual," [Online].
- [8] Occupational Safety and Health Administration, "METHYL ALCOHOL (METHANOL)," [Online].
- [9] G. Pasini, F. Bollentini, F. Tocchi and L. Ferrari, "Assessing the Potential of Hybrid Systems with Batteries, Fuel Cells and E-Fuels for Onboard Generation and Propulsion in Pleasure Vessels," *Energies*, no. 17, p. 6416, 2024.
- [10] Sanlorenzo spa, "Progetto Life Mystic," [Online]. Available: https://www.sanlorenzoyacht.com/it/sviluppo-responsabile/progetto-life-mystic.asp.
- [11] J. Perry, D. W. Green and M. W. Southard, Perry's Chemical Engineers' Handbook, Mc Graw Hill, 2018.
- [12] C. De Boom, A. W. Vredeveldt, A. van Hoeve, L. van Biert, A. J. Bottger and I. Akkerman, "The underwater ventilation of methanol vapour," 2023.
- [13] Siemens, "User Guide on Support center Siemens," [Online]. Available: https://support.sw.siemens.com/it-IT.
- [14] D. Ramkrishna, Population balances, Academic Press, 2000.
- [15] S. Lo and D. Zhang, "Modelling of Break-up and Coalescence in Bubbly Two-Phase Flows," *J. Comp. Multiphase Flows*, vol. 1, no. 1, pp. 23-38, 2009.
- [16] G. Cerne, S. Petelinb and I. Tiselja, "Coupling of the Interface Tracking and the Two-Fluid Models for the Simulation of Incompressible Two-Phase Flow," *Journal of Computational Physics*, vol. 171, no. 2, pp. 776-804, 2001.
- [17] W. E. Ranz and W. R. Marshall, "Evaporation from drops--Part I and II," *Chemical Engineering Progress*, vol. 48, no. 3, p. 141, 1952.
- [18] *DIN EN 590*.
- [19] Global, "Safety Datasheet Diesel Fuel," [Online].